The object of this study was the motion of an ultralight class variable-length launch vehicle made of a polymer body along the active phase of the trajectory. The work considers the solution to the problem of designing low-cost means of delivery to orbit, namely to the assessment of the possibility of removing the payload by a carrier rocket with a polymer body of variable length beyond the dense atmosphere of the Earth. For this purpose, ballistic projection of the trajectory of the launch vehicle was carried out taking into account overloading; its aerodynamic characteristics and peculiarities of aerothermodynamic processes occurring during flight in the atmospheric phase of the trajectory were determined. The closeness (up to 10 %) of the obtained results with known experimental data is shown. The influence of the aerodynamic force on the parameters of the launch vehicle motion was studied. A flight simulation was conducted, the results of which showed the fundamental possibility of launching a CubeSat 24U class payload using a launch vehicle with a polymer body of variable length to a suborbital trajectory with an altitude of about 300 km. At the same time, the effective longitudinal overload on the body of the launch vehicle does not exceed 4 units, and the temperature on the surface of the body does not exceed 300 K. A feature of the research is the use of a multidisciplinary approach, which implies taking into account the interrelationship of aerodynamic, thermodynamic, and ballistic processes. The established motion parameters, aerodynamic characteristics, and the surface heating temperature of the launch vehicle body are key values for further research on the design and analysis of a launch vehicle with a polymer body of variable length. These data could be used to calculate the mechanical and thermal loads acting on the structure of the launch vehicle during flight

Keywords: launch vehicle, variable length, polymer body, aerodynamic characteristics, suborbital trajectory

UDC 629.764.7
DOI: 10.15587/1729-4061.2024.306225

ASSESSING THE POSSIBILITY OF USING A VARIABLE-LENGTH LAUNCH VEHICLE WITH A POLYMER BODY FOR ORBITING PAYLOAD

Aleksandr Golubek
Corresponding author
Doctor of Technical Sciences, Professor
Department of Cyber Security
and Computer-Integrated Technologies*
E-mail: holubek@ftf.dnu.edu.ua
Serhii Aleksieienko
Doctor of Technical Sciences, Professor
Department of Mechanical Engineering Technology
and Materials Science
Dnipro University of Technology
Dmytra Yavornytskoho ave., 19, Dnipro, Ukraine, 49005
Mykola Dron
Doctor of Technical Sciences, Professor
Department of Rocket and Space and Innovative Technologies*
Andrii Dreus
Doctor of Technical Sciences, Professor
Department of Fluid Mechanics and Energy and Mass Transfer*
*Oles Honchar Dnipro National University
Nauky ave., 72, Dnipro, Ukraine, 49010

Received date 29.03.2024
Accepted date 14.06.2024
Published date 28.06.2024

How to Cite: *Golubek, A., Aleksieienko, S., Dron, M., Dreus, A. (2024). Assessing the possibility of using a variable-length launch vehicle with a polymer body for orbiting payload. Eastern-European Journal of Enterprise Technologies, 3 (7 (129)), 63–72. https://doi.org/10.15587/1729-4061.2024.306225*

1. Introduction

Analysis of modern trends in the development of rocket and space technology reveals a sustained interest in variable-length polymer launch vehicles (LVs). The stage body of such launch vehicles is simultaneously the fuel used to generate the jet thrust necessary to overcome the Earth's gravity and provide access to near-Earth space. Owing to these qualities, it is possible to achieve a simplification of the design, a reduction in the cost of launching the LV, as well as an increase in the environmental friendliness of the removal process due to the minimization of the number of design elements that are separated and reach the Earth's surface.

The use of polymeric materials for LV as structural materials has a number of features. In particular, they differ significantly in their mechanical and physicochemical properties from classic metal alloys. This necessitates the search for optimal trajectories of motion to prevent the possible negative impact of mechanical and thermal loads on the active atmospheric phase of the flight path.

The main parameter characterizing the magnitude of the operating mechanical loads on the LV body is the magnitude of the overload, which varies with flight time. At the same time, the body's ability to withstand mechanical loads is characterized by the values of the Young's modulus, as well as the temperature-dependent limits of strength and yield of the material. Thermal loads are due to aerodynamic heating of the outer surface of the LV housing due to the action of the aerodynamic resistance force of the dense layers of the atmosphere.

In addition, it should be noted that the variability of the length of LV along the active part of the trajectory is atypical for classic LVs, in the design of which the influence of the aerodynamic resistance of the Earth's atmosphere is usually taken into account using aerodynamic force factors, which are functions of the angle of attack, Mach number, and flight

altitude. In turn, another variable parameter appears in the LV of variable length – the length, which monotonically decreases during the flight. Therefore, the nature of influence of the aerodynamic resistance of the atmosphere on the flight of a variable-length LV along the active phase of the trajectory will differ from that of classic LVs.

From the above, it follows that the issue of designing polymer LVs of the ultralight class of variable length is relevant.

2. Literature review and problem statement

The task of designing a variable-length LV is related to the development of a new type of promising LVs that use polymers as a structural material for the body. The state of the issue and the main problems that arise during the development of such LVs are highlighted in a number of works [1–9], which are a priority in this direction. The results of those studies testify to the multidisciplinary and multifaceted nature of the task of creating an ultralight polymeric LV. Paper [1] proposed the concept of using this type of LV as a means of launching small satellites. The design of a variable-length single-stage LV with a polyethylene body is proposed but the attention is focused on the problem of creating a suitable propulsion system (PS), while the issue of the reliability of the body is not considered. Work [2] presents the concept of a variable-length picorocket, which makes it possible to launch a payload weighing 1 kg into Earth orbit. However, the authors theoretically justify the possibility of creating such a rocket without taking into account the dynamic and thermal loads that occur in the atmospheric phase of the trajectory. Paper [3] reports the results of a successful terrestrial experimental development of an autophagic PS, which opens up the possibility of creating a real LV with a polymer body. In this regard, the problem of studying aerothermodynamic processes for bodies that change elongation during motion is actualized. In work [4], the main issues of designing a variable-length LV for the launch of service vehicles are considered, and the problem of aerothermodynamics research is formulated in a general way, but only from the point of view of the return of spacecraft into the atmosphere. It should be noted that under the return mode the loads are significantly different from the device start mode. Trajectories of motion, modes of operation of PS, and patterns of changes in body length, in the case of using autophagic LVs, are presented in works [5, 6]. But it should be noted that under the conditions of changes in the elongation of the body, the aerodynamic characteristics also change, which must be taken into account to determine the design parameters. An experimental study [7] testifies to sufficiently high temperatures of the structure of the PS during operation, but the issue of the temperature on the surface of the housing is not studied. These issues are considered in [8] within the framework of the problem of thermal conductivity for the case but without taking into account the interaction with the external high-speed gas flow. A similar problem, taking into account mechanical phenomena was considered in work [9], in which the principal possibility of using polymer materials (polyethylene, polypropylene) as structural materials for the LV body is substantiated. But the question of changing the boundary conditions on the surface of the hull during the motion of the LV remains open. A possible way to solve the problem of ensuring heat resistance of housings is the use of composite polymer materials [10]. But in this case, the problem of effective use of such materials as fuel in autophagic PS requires research. Such materials can be effectively used in structural elements of the main fairing (MF) [11], or in composite sandwich structures with cellular filler [12]. However, the issue of their effective disposal in PS has not yet been studied. At the same time, pure or metallized polymers provide high energy characteristics of solid-fuel rocket launchers [13], and theoretically make it possible to achieve high specific impulses but are sensitive from the point of view of thermal and heat resistance [14].

So, the above studies prove the prospect of using polymeric materials to design a new type of LV but leave out a number of important issues. In particular, regarding the determination of the loads acting on LV in the active phase of the trajectory on the polymer hulls, as well as the influence of the variability of hull geometry on the aerodynamic characteristics.

The complexity of this research is unconditional and requires the involvement of a large number of highly qualified specialists with different profiles. The first step on this path is to determine the motion parameters and aerothermodynamic processes of the active phase of LV trajectory. Its results are the input data for the task of researching the integrity of the LV structure under the conditions of mechanical and thermal loads. All this gives reason to assert that it is expedient to conduct a study on the parameters of LV motion and aerothermodynamic processes on the active phase of LV trajectory.

3. The aim and objectives of the study

The purpose of our work is to assess the possibility of taking the payload from the dense atmosphere of the Earth by using an ultra-light variable-length LV from a polymer body. This requires conducting ballistic projection of LV trajectory, taking into account the peculiarities of aerothermodynamic processes in the atmospheric area. This will provide an opportunity to conduct a study on the integrity of LV structure under the conditions of mechanical and thermal loads of the active phase of the trajectory.

To this end, it is necessary to solve the following tasks:

– to construct a mathematical model of LV motion along the active phase of the trajectory, taking into account aerothermodynamic effects;

– to investigate aerothermodynamic processes during the motion of LV in the atmospheric area and to determine the dynamic and temperature regimes of LV;

– to evaluate the power of LV to launch the CubeSat 24U class payload into a suborbital trajectory that goes beyond the dense layers of the Earth's atmosphere.

4. The study materials and methods

The object of our study is the motion of a variable-length ultralight class LV made of a polymer body along the active phase of the trajectory.

The main hypothesis of the research assumes the possibility of reaching by a variable-length ultralight class LV from a polymer body a flight altitude outside the dense layers of the Earth's atmosphere. At the same time, a specified level of mechanical (longitudinal overload of 4 units) and thermal (320–370 K) load on the LV housing will be provided.

The following assumptions were adopted:

– LV is a solid body of variable mass and variable length, moving under the action of thrust forces, the Earth's gravity, and the aerodynamic force;

– the LV stabilization system is ideal;

– Earth is general terrestrial ellipsoid WGS-84;

– the gravitational potential of the Earth takes into account the influence of the 2nd, 3rd, and 4th zonal harmonics;

– Earth's atmosphere is standard (MFST 4401–81. Standard atmosphere. Parameters);

– PS of LV is ideal and has perfect regulation;

– the output is for a payload with a standard size of CubeSat 24U;

– we do not take into account the change in the mechanical characteristics of the housing in the first approximation;

– the starting point (SP) is set by the geocentric latitude, longitude, and altitude, which are equal to zero; launch azimuth is 90°.

An ultra-light class rocket of variable length made of a polymer body with the effect of autophagy, which is proposed in [4], is considered as a launch vehicle. Its characteristics:

– body material – polyethylene;

– starting mass, fuel mass, and mass of the final structure with payload and control system are 300 kg, 250 kg, and 50 kg, respectively;

– the vacuum thrust, specific impulse, and target section of jet pipe of PS are 8000 N, 200 s, and 0.05 m^2, respectively;

– initial length 6.1 m; final length 2.38 m; fuel length 3.72 m; length of PS 1.45 m; length of MF 0.93 m.

– the diameter of LV is 0.3 m.

A fairly wide range of methods is used to calculate the aerodynamic characteristics of an aircraft moving at speeds ranging from subsonic to supersonic. They can be conventionally divided into engineering methods, which are largely based on empirical relationships, and theoretical methods, which are based on solving the Navier-Stokes equations.

Most published results from calculating the aerodynamic characteristics of LV were obtained using approximate engineering methods, for example, [15], or methods from linear potential theory, such as [16–18].

The results of calculations of high-speed rarefied flows in works [19, 20] were obtained using the Petrov-Galerkin compressible flow method, supplemented by the capture of YZβ shock waves, and using a unified gas kinetic scheme and direct simulation by the Monte Carlo method. The method of surface elements was used to calculate the aerodynamic characteristics of hypersonic vehicles in [21].

The aerodynamic characteristics of the complete layout of LV are obtained using methods based on Newton's theory, for example, [22], which, however, is focused on high supersonic and hypersonic speeds. Also, an approximate calculation of the supersonic flow around LV can be performed using the numerical integration of the Euler equations [23, 24]. Numerical solutions to these equations make it possible to estimate, however, without taking into account viscosity, the magnitude of aerodynamic forces and moments, the distribution of loads on the load-bearing elements of the hull. Moreover, numerical methods, in general, do not require the involvement of empirical results. They make it possible to get information about the state of the current in the entire calculation area. This is too complicated for experimental research methods and practically impossible for semi-empirical methods. As noted, viscous effects, such as, for example, the shedding of vortices from the rocket body, cannot be accounted for using Euler's equations alone. Therefore, in order to determine their impact, specific methods, which depend on the class of currents, can be additionally applied.

It should be noted that since the methods listed above are characterized by rather strict restrictions on their application, this complicates their practical use in the study of aerodynamics of LV. The solution to this problem can be the use of methods of computational hydrodynamics, which are based on solving the difference analogs of the nonlinear equations of gas dynamics the Navier-Stokes equations, in full or simplified form. Such a model of fluid and gas mechanics makes it possible to more accurately describe the physical processes that occur when flowing around the aerodynamic surfaces of LV, such as the formation of a shock wave, turbulence, flow separation, eddy currents, thermal loads, etc. [25].

To achieve the goal, the problem was considered in the form of two successive iterations. The first consists of modeling the flight of LV without taking into account the influence of the Earth's atmosphere. According to its results, the following dependences on time are determined:

– atmospheric velocity;

– flight altitude;

– atmospheric pressure;

– atmospheric temperature;

– atmospheric density;

– speed of sound;

– angles of attack;

– the length of LV, etc.

With the use of these data, the aerothermodynamic processes during the motion of LV in the atmospheric area are studied and the dynamic and temperature regimes of LV are determined, in particular:

– aerodynamic force factors are determined;

– the temperature on the surface is determined on the stage of LV.

The second iteration is the simulation of LV flight taking into account the influence of the Earth's atmosphere. According to its results, the energy capabilities of LV to launch the payload into near-Earth orbits are determined.

5. Results of assessing the possibility of using a polymer launch vehicle of the ultralight class

5. 1. Construction of a mathematical model of the launch vehicle motion taking into account aerothermodynamic effects

5. 1. 1. Mathematical model of the motion of the launch vehicle along the active phase of the trajectory

To assess the possibility of launching the payload into Earth orbit and determining the surface temperature of LV body, a mathematical motion model was built.

Three coordinate systems are considered:

1. The initial starting geocentric coordinate system (ISCS) $O_0X_0Y_0Z_0$. The center of this right orthogonal inertial coordinate system is located at the center of the Earth. The O_0Y_0 axis is parallel to the normal to the Earth's surface in SP and is directed from the center of the Earth. The O_0X_0 axis lies in a plane parallel to the plane of the local horizon in SP, and forms an angle with the north direction in the SP equal to the launch azimuth of LV. The O_0Z_0 axis complements the coordinate system to the right.

2. The coordinate system (COCS) $O_1X_1Y_1Z_1$ is related to the center of mass (CM) of LV. This is a non-inertial right orthogonal coordinate system with the center in the CM of LV. The O_1X_1 axis is parallel to the longitudinal axis of LV and is directed in the direction of its nose. The O_1Y_1 axis lies in the plane of normal stabilization and is directed in the direction of stabilizer III. The O_1Z_1 axis complements the coordinate system to the right.

3. WGS-84 coordinate system. The center of this non-inertial right orthogonal coordinate system $O_WX_WY_WZ_W$ coincides with the center of the Earth. The O_WX_W axis lies in the plane of the equator and is directed in the direction of the WGS-84 zero meridian. The O_WZ_W axis coincides with the angular velocity vector of the Earth's daily rotation. The O_WY_W axis complements the coordinate system to the right.

Taking into account the introduced assumptions, the mathematical model of motion is represented in the following form:

$$\begin{bmatrix}\dot V_{X_0}\\ \dot V_{Y_0}\\ \dot V_{Z_0}\end{bmatrix}=\begin{bmatrix}\dot W_{X_0}\\ \dot W_{Y_0}\\ \dot W_{Z_0}\end{bmatrix}+\begin{bmatrix}g_{X_0}\\ g_{Y_0}\\ g_{Z_0}\end{bmatrix}, \quad (1)$$

$$\begin{bmatrix}\dot R_{X_0}\\ \dot R_{Y_0}\\ \dot R_{Z_0}\end{bmatrix}=\begin{bmatrix}V_{X_0}\\ V_{Y_0}\\ V_{Z_0}\end{bmatrix}, \quad (2)$$

$$\begin{bmatrix}\dot\lambda_0\\ \dot\lambda_{X_1}\\ \dot\lambda_{Y_1}\\ \dot\lambda_{Z_1}\end{bmatrix}=\frac{1}{2}\begin{bmatrix}-\lambda_{X_1}\omega_{X_1}-\lambda_{Y_1}\omega_{Y_1}-\lambda_{Z_1}\omega_{Z_1}\\ \lambda_0\omega_{X_1}+\lambda_{Y_1}\omega_{Z_1}-\lambda_{Z_1}\omega_{Y_1}\\ \lambda_0\omega_{Y_1}-\lambda_{X_1}\omega_{Z_1}+\lambda_{Z_1}\omega_{X_1}\\ \lambda_0\omega_{Z_1}+\lambda_{X_1}\omega_{Y_1}-\lambda_{Y_1}\omega_{X_1}\end{bmatrix}, \quad (3)$$

$$\dot m=-\dot m_{EN}, \quad (4)$$

$$\dot l=-\dot l_{EN}, \quad (5)$$

where V_{X_0}, V_{Y_0}, V_{Z_0} are the projections of the vector of absolute velocity of LV CM on the axis of ISCS; W_{X_0}, W_{Y_0}, W_{Z_0} – projections of the vector of apparent velocity of LV CM on the axis of ISCS; g_{X_0}, g_{Y_0}, g_{Z_0} – projections of the acceleration vector of the Earth's gravity in the CM of LV on the axis of ISCS; R_{X_0}, R_{Y_0}, R_{Z_0} – vector projections of the current position of LV CM on the axis of the ISCS; λ_0, λ_{X_1}, λ_{Y_1}, λ_{Z_1} – elements of the quaternion of the orientation of LV relative to ISCS; ω_{X_1}, ω_{Y_1}, ω_{Z_1} – projections of the angular velocity vector of LV around CM on the COCS axis; m – current mass of LV; $\dot m_{EN}$ – mass flow rate of PS; l – current length of LV; $\dot l_{EN}$ – the rate of change in the length of LV.

Projections of the apparent acceleration vector onto the axis of ISCS are defined as:

$$\begin{bmatrix}\dot W_{X_0}\\ \dot W_{Y_0}\\ \dot W_{Z_0}\end{bmatrix}=\frac{1}{m}M_{X_0\leftarrow X_1}\begin{bmatrix}P+S_{X_1}\\ S_{Y_1}\\ S_{Z_1}\end{bmatrix}, \quad (6)$$

$$M_{X_0\leftarrow X_1}=\begin{pmatrix}2\left(\lambda_0^2+\lambda_{X_1}^2\right)-1 & 2\left(\lambda_{X_1}\lambda_{Y_1}-\lambda_0\lambda_{Z_1}\right) & 2\left(\lambda_{X_1}\lambda_{Z_1}+\lambda_0\lambda_{Y_1}\right)\\ 2\left(\lambda_{X_1}\lambda_{Y_1}+\lambda_0\lambda_{Z_1}\right) & 2\left(\lambda_0^2+\lambda_{Y_1}^2\right)-1 & 2\left(\lambda_{Y_1}\lambda_{Z_1}-\lambda_0\lambda_{X_1}\right)\\ 2\left(\lambda_{X_1}\lambda_{Z_1}-\lambda_0\lambda_{Y_1}\right) & 2\left(\lambda_{Y_1}\lambda_{Z_1}+\lambda_0\lambda_{X_1}\right) & 2\left(\lambda_0^2+\lambda_{Z_1}^2\right)-1\end{pmatrix}, \quad (7)$$

where $M_{X_0\leftarrow X_1}$ is the transition matrix from COCS to ISCS; P – thrust force of LV PS; S_{X_1}, S_{Y_1}, S_{Z_1} – longitudinal, normal, and cross-section components of the aerodynamic force.

Let's determine the thrust force of LV PS:

$$P=P_0-S_{SC}p_A, \quad (8)$$

where P_0 – vacuum thrust of PS; S_{SC} – target section of jet pipe of PS; p_A is the pressure of the Earth`s atmosphere.

Pressure p_A, speed of sound c_A, and density ρ_A of the Earth's atmosphere according to MFST 4401–81 are functions of flight altitude h. It, in turn, depends on the vector of the current position of LV CM. To determine the flight altitude according to [26] the projection of the current position vector on the axis of the WGS-84 coordinate system:

$$\begin{bmatrix}R_{X_W}\\ R_{Y_W}\\ R_{Z_W}\end{bmatrix}=M_{X_W\leftarrow X_0}\begin{bmatrix}R_{X_0}\\ R_{Y_0}\\ R_{Z_0}\end{bmatrix}, \quad (9)$$

$$M_{X_W\leftarrow X_0}=\begin{pmatrix}-\sin\varphi_{g_0}\cos\eta\cos A_0-\\ -\sin\eta\sin A_0 & \cos\varphi_{g_0}\cos\eta & \sin\varphi_{g_0}\cos\eta\sin A_0-\\ & & -\sin\eta\cos A_0\\ -\sin\varphi_{g_0}\sin\eta\cos A_0+\\ +\cos\eta\sin A_0 & \cos\varphi_{g_0}\sin\eta & \sin\varphi_{g_0}\sin\eta\sin A_0+\\ & & +\cos\eta\cos A_0\\ \cos\varphi_{g_0}\cos A_0 & \sin\varphi_{g_0} & -\cos\varphi_{g_0}\sin A_0\end{pmatrix}, \quad (10)$$

$$\eta=\lambda_{g_0}-\omega_E t, \quad (11)$$

where $M_{X_W\leftarrow X_0}$ is the transition matrix from ISCS to the WGS-84 coordinate system; φ_{g_0} – geodetic latitude of SP; λ_{g_0} – geodetic longitude of SP; A_0 – launch azimuth; ω_E – angular velocity of the Earth's daily rotation; t is the time from the moment of launch.

The components of the aerodynamic force vector are found from the ratios:

$$S_{X_1}=-qS_MC_X\alpha_S, \quad (12)$$

$$S_{Y_1}=-qS_MC_Y^\alpha\alpha, \quad (13)$$

$$S_{Z_1}=-qS_MC_Z^\beta\beta, \quad (14)$$

where q is the high-speed pressure; S_M – midsection area; C_X^α, C_Y^α, C_Z^β – aerodynamic force factors; α_S, α, β – spatial angle of attack, angle of attack, and angle of slip, respectively.

To determine the high-speed pressure, aerodynamic force factors , and angles of attack, projections of the vector of the atmospheric velocity onto the axis of ISCS were found:

$$\begin{bmatrix}V_{rX_0}\\ V_{rY_0}\\ V_{rZ_0}\end{bmatrix}=\begin{bmatrix}V_{X_0}-\omega_E\left(R_{Z_0}\sin\varphi_{g_0}+R_{Y_0}\cos\varphi_{g_0}\sin A_0\right)\\ V_{Y_0}-\omega_E\left(-R_{X_0}\cos\varphi_{g_0}\sin A_0-R_{Z_0}\cos\varphi_{g_0}\cos A_0\right)\\ V_{Z_0}-\omega_E\left(R_{Y_0}\cos\varphi_{g_0}\cos A_0-R_{X_0}\sin\varphi_{g_0}\right)\end{bmatrix}. \quad (15)$$

The high-speed pressure is calculated from the expressions:

$$q = \frac{\rho_A V_r^2}{2}, \tag{16}$$

$$V_r = \sqrt{V_{rX_0}^2 + V_{rY_0}^2 + V_{rZ_0}^2}. \tag{17}$$

The angles of attack and slip are determined from the equations:

$$\alpha = -\text{arctg}\left(\frac{V_{rY_1}}{V_{rX_1}}\right), \tag{18}$$

$$\beta = \arcsin\left(\frac{V_{rZ_1}}{V_r}\right), \tag{19}$$

$$\alpha_S = -\arccos\left(\frac{V_{rX_1}}{V_r}\right), \tag{20}$$

$$\begin{bmatrix} V_{rX_1} \\ V_{rY_1} \\ V_{rZ_1} \end{bmatrix} = M^T_{X_0 \leftarrow X_1} \begin{bmatrix} V_{rX_0} \\ V_{rY_0} \\ V_{rZ_0} \end{bmatrix}. \tag{21}$$

The aerodynamic force factors are functions of the Mach number, the length of LV, and its shape. The Mach number is determined by the ratio:

$$M_\infty = \frac{V_r}{c_A}. \tag{22}$$

Projections of the acceleration vector of the Earth's gravity in the CM of LV on the axis of ISCS, taking into account the accepted assumptions, are determined by the equations:

$$\begin{bmatrix} g_{X_0} \\ g_{Y_0} \\ g_{Z_0} \end{bmatrix} = \frac{g_r}{R} \begin{bmatrix} R_{X_0} \\ R_{Y_0} \\ R_{Z_0} \end{bmatrix} + g_\omega \begin{bmatrix} \cos\varphi_{g_0} \cos A_0 \\ \sin\varphi_{g_0} \\ -\cos\varphi_{g_0} \sin A_0 \end{bmatrix}, \tag{23}$$

$$g_r = -\frac{\mu}{R^2} \times \left\{ \begin{array}{l} 1 + \frac{3}{2}\frac{a_E^2}{R^2} C_{2,0}\left(5\sin^2\varphi_E - 1\right) + \\ + \frac{5}{2}\frac{a_E^3}{R^3} C_{3,0} \sin\varphi_E \left(7\sin^2\varphi_E - 3\right) + \\ + \frac{15}{8}\frac{a_E^4}{R^4} C_{4,0}\left[7\sin^2\varphi_E \left(3\sin^2\varphi_E - 2\right) + 1\right] \end{array} \right\} \times, \tag{24}$$

$$g_\omega = \frac{\mu}{R^2} \left\{ \begin{array}{l} 3\frac{a_E^2}{R^2} C_{2,0} \sin\varphi_E + \\ + \frac{3}{2}\frac{a_e^3}{R^3} C_{3,0}\left(5\sin^2\varphi_E - 1\right) + \\ + \frac{5}{2}\frac{a_E^4}{R^4} C_{4,0} \sin\varphi_E \left(7\sin^2\varphi_E - 3\right) \end{array} \right\}, \tag{25}$$

$$R = \sqrt{R_{X_0}^2 + R_{Y_0}^2 + R_{Z_0}^2}, \tag{26}$$

$$\sin\varphi_E = \frac{R_{Z_W}}{R}, \tag{27}$$

where μ – gravitational constant; a_E – semimajor axis of the general terrestrial ellipsoid; $C_{2,0}$, $C_{3,0}$ and $C_{4,0}$ – coefficients of the Earth's gravitational potential.

The rate of change in LV length:

$$\dot{l}_{EN} = \frac{\dot{m}_{EN}}{\rho_B S_B}, \tag{28}$$

where ρ_B – fuel density; S_B – cross-sectional area of the fuel.

5. 1. 2. Mathematical model of aerothermodynamic processes during the motion of LV in dense layers of the atmosphere

To simulate the external air flow during subsonic, transonic, and supersonic flow around an ultralight class LV, we use the Reynolds-averaged Navier-Stokes equations, which can be written in vector form:

$$\frac{\partial \overline{q}}{\partial t} + \frac{\partial \overline{E}_i}{\partial x_i} = 0, \tag{29}$$

$$\overline{q} = \begin{bmatrix} \rho \\ \rho_A u_1 \\ \rho_A u_2 \\ \rho_A u_3 \\ e \end{bmatrix},$$

$$\overline{E}_i = \begin{bmatrix} \rho_A u_i \\ \rho_A u_i u_1 + \delta_{1i} p_A - \tau_{1i} \\ \rho_A u_i u_2 + \delta_{2i} p_A - \tau_{2i} \\ \rho_A u_i u_3 + \delta_{3i} p_A - \tau_{3i} \\ \left(e + p_A\right) u_i - u_j \tau_{ij} - q_i \end{bmatrix}, \tag{30}$$

where t is time; x_i – Cartesian coordinates; u_i – Cartesian components of the velocity vector; i, j=1, 2, 3 – indices; e – total energy; τ_{ij} – components of the shear stress tensor; q_{ij} – the components of the heat flow vector [27–31].

To close the system of equations (29), (30), you can use the SST (Shear Stress Transport) turbulence model, which is a combination of the standard k–ε model and the Wilcox k–ω model. It should be noted that the k–ε model has proved effective in the calculation of free and jet shear flows. In turn, the k–ω model describes the near-wall boundary layers well [32–36].

The spatial model of the calculation area is chosen in the form of a combined paraboloid, which makes it possible to reduce the number of nodes during the subsequent construction of the calculation grid. In the middle of the paraboloid, there is a geometric model of LV, which consists of a cone-shaped or oval-shaped MF and a cylindrical stage. The relative size of the calculation area is chosen so that the distance from the streamlined body to the outer boundary is ~20–25 lengths of the streamlined body. Using an unstructured calculation grid, the calculation area of the mathematical modeling of the flow around LV consisted of 1302016 control volumes (Fig. 1). Polyhedral cells were used in the construction of the grid because compared to tetrahedral or hybrid grids, this makes it possible to significantly reduce the total number of cells. Accordingly, the

use of polyhedral cells makes it possible to obtain a higher accuracy of the solution. Increasing the number of cell connections improves the convergence of the calculation process compared to a triangular mesh, while reducing the calculation time (compared to a triangular mesh with equivalent accuracy).

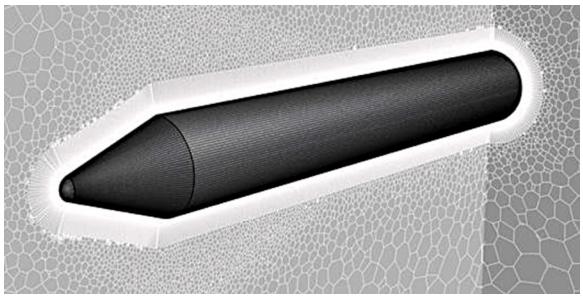

Fig. 1. Design grid for simulation

The calculation mesh was thickened to the streamlined surface in such a way that the minimum step of the near-wall mesh satisfied the condition $y^+<0.4$, where y^+ is the dimensionless thickness of the viscous sublayer:

$$y^+ = \frac{u_\tau \Delta y_1}{\nu},$$

where $u_\tau = \sqrt{\frac{\tau_W}{\rho_A}}$ is the friction velocity; $\tau_W = \frac{C_f \rho_A u^2}{2}$ – wall shear stress; $C_f = \frac{0.058}{\mathrm{Re}^{0.2}}$ – skin friction coefficient; Δy_1 – absolute distance from the wall; v – kinematic viscosity; Re is the Reynolds number.

As a test, the problem of flowing around the aerodynamic shape of the pointed nose parts of LV was considered. To verify the results, known experimental data published in the work "Aerodynamics of bodies of the simplest shapes" were chosen.

5. 2. Investigating aerothermodynamic processes during the motion of a launch vehicle

To take into account the influence of the atmosphere on the dynamics of the flight of LV with a polymer body, a numerical study of aerodynamic and thermophysical processes in the atmospheric phase was carried out. Fig. 2 shows the calculated and experimental [37] dependences of the longitudinal aerodynamic force factor of MF C_{X0} on the Mach number of the oncoming flow at zero angle of attack. The first are indicated by a solid line, the second by circular markers. The research was conducted in the range from subsonic (M_∞=0.2) to supersonic speeds (M_∞=4). Conical (Fig. 2, *a*) and ogive (Fig. 2, *b*) shapes of MF with lengths of 2.57*d*, 1.54*d*, and 0.865*d* were considered, where *d* is the diameter of the cylindrical part. The length of LV stage is taken as 7*d*.

The structure of the flow around LV for different flight speeds is shown in Fig. 3. Calculations were performed for subsonic (Mach number for the oncoming flow M_∞=0.6), transonic (M_∞=1.0), and supersonic flow regimes (M_∞=1.2). The results are shown as local Mach number fields.

The data in Fig. 3 demonstrate the pattern in the formation of local supersonic zones and the formation of shock-waves with increasing oncoming flow velocity. Figures 4–6 show the results of calculating LV longitudinal aerodynamic force factor and temperature for the conditions corresponding to 83 s of flight at an altitude of 13.3 km, where the maximum heat flow $\left(\frac{\rho_A V_r^3}{2}\right)$ is observed. Air temperature – 216.7°K, pressure – 15795 Pa, relative flight speed – 749.17 m/s (M_∞=2.54), LV length – 12.3*d*.

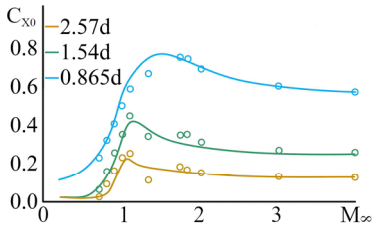

a

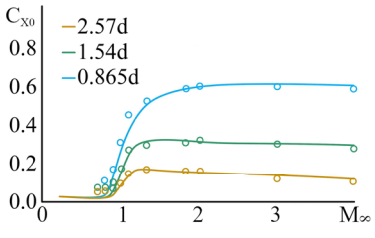

b

Fig. 2. Influence of the Mach number, shape, and length of the main fairing of a launch vehicle on the longitudinal aerodynamic force factor: *a* – conical shape; *b* – ogive form

a

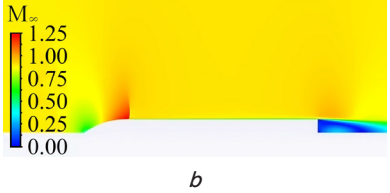

b

c

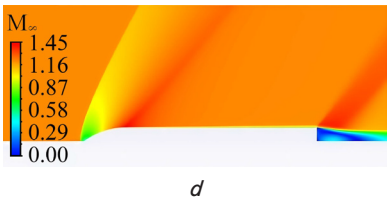

d

Fig. 3. Patterns of the launch vehicle flow structure depending on the Mach number for the ogive main fairing (length 1.54*d*): *a* – M_∞=0.6; *b* – M_∞=0.9; *c* – M_∞=1.0; *d* – M_∞=1.2

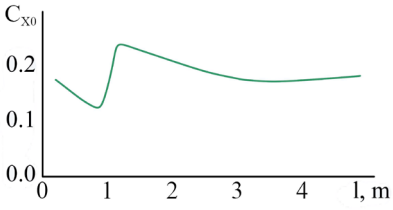

Fig. 4. Dependence of the longitudinal aerodynamic force factor of a launch vehicle on the Mach number of the oncoming flow for the considered calculation case

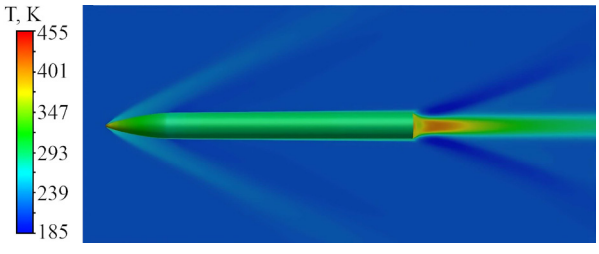

Fig. 5. Temperature distribution of the flow around the streamlined shape of a launch vehicle

The obtained data were used to assess the possibility of launching the payload into a suborbital trajectory, taking into account the influence of the atmosphere.

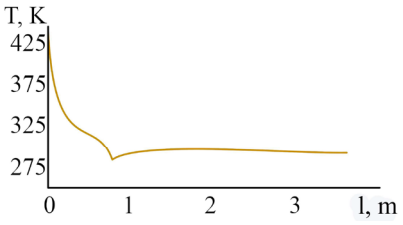

Fig. 6. Wall temperature distribution along the streamlined shape of a launch vehicle

5. 3. Assessing the energy capacity of a launch vehicle for launching the payload of the CubeSat 24U class into a suborbital trajectory

As a result of our computer simulation using the motion model (1) to (28), the dependences of the trajectory parameters of LV on the flight time were established.

The simulation was carried out for two calculation cases:

– without taking into account the influence of the aerodynamic force to determine the dependence of the aerodynamic force factors on the parameters of the Earth's atmosphere and LV according to the flight time;

– taking into account the aerodynamic force.

As a result of the computer simulation using the motion model (1) to (28), the dependences of the trajectory parameters of LV on the flight time were derived (Fig. 7).

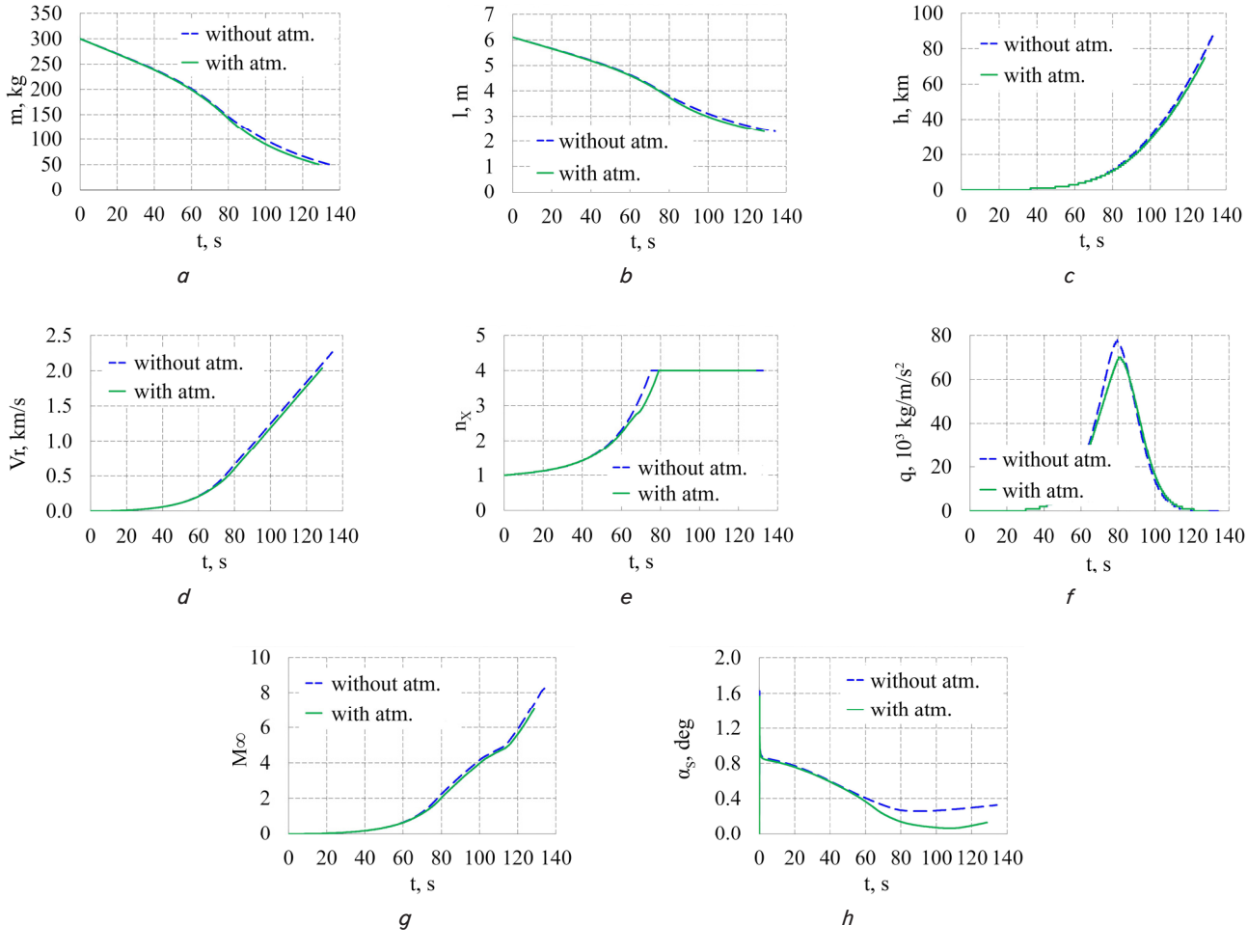

Fig. 7. Dependence of launch vehicle parameters on flight time: *a* – mass; *b* – length; *c* – altitude; *d* – atmospheric velocity; *e* – longitudinal overload; *f* – high-speed pressure; *g* – Mach number; *h* – angle of spatial attack

The data in Fig. 7 make it possible to assess the influence of the atmosphere on the design parameters, which, in turn, is the basis for developing a rational flight program for LV.

6. Discussion of results of investigating the possibility of using a polymer launch vehicle of ultralight class

As can be seen from the data in Fig. 2, the shape and length of MF exert a significant effect on the aerodynamic resistance of LV, which increases at transonic speeds, where wave resistance plays a significant role. Especially sharp changes occur for configurations of cylindrical bodies with conical nasal parts with a large angle at the top (Fig. 2, *a*). Wave resistance occurs at high subsonic velocities (M_∞>0.9) on the long-length ogive MF, and its increase occurs less intensively (Fig. 2, *b*). Further transition from subsonic to supersonic speeds in certain cases is accompanied by a sharp change in aerodynamic characteristics at small angles of attack. If you compare the resistance of the ogive and conical MF, the resistance of the first for the same length is smaller. This difference is most observed for short-length MF.

From the data in Fig. 2, it turns out that the obtained calculated values correlate well with the experimental data [37]. For the most part, their deviation does not exceed 10 %, except in the region of Mach numbers 1.2–1.3. This can be explained by errors in the measurement process.

Fig. 3 illustrates the dependence of the structure of the flow around LV and the features of the flow in the subsonic, transonic, and supersonic regimes at zero angle of attack. At low subsonic speeds (Fig. 3, *a*) and Reynolds numbers corresponding to the range of calculated parameters, the frontal drag almost does not depend on the number M_∞ (it will depend only on the angle of attack). When the speed of the oncoming flow increases to reach the local speed of sound, the frontal resistance begins to increase due to the occurrence of the so-called wave resistance. This is due to the occurrence of compression jumps that close the formed local supersonic zones (Fig. 3, *b*). The dependence of the longitudinal aerodynamic force factor on the Mach number for specific flight conditions (Fig. 4), where maximum heat loads are expected, show that a sharp increase in aerodynamic resistance is observed in the transonic region. Therefore, the transition from subsonic to supersonic modes, which takes place in the atmospheric phase, must be taken into account when calculating the trajectory.

The temperature calculation data (Fig. 5, 6) show that the main temperature loads at supersonic velocities take place on LV MF. The temperature behind the sealing jumps on the surface of the hull of LV stage does not exceed 300 K, in contrast to [38], in which aerodynamic heating leads to an increase in the temperature of the aircraft hull (which moves with M=3.5 at an altitude of 15 km) to values of ~450 K. The obtained temperature distribution on the streamlined surface allows us to conclude about the acceptability of using polymers as a structural material of ultra-light class LVs. In addition, taking into account the fact that the strength characteristics of polymer materials, in particular polyethylene, are quite sensitive to temperature. This becomes possible owing to the selection of flight parameters of LV in the dense layers of the atmosphere, in particular, the setting of an overload limit at 4 units.

In order to obtain data for further design, aerodynamic calculations of the variable-length ultralight class LV were carried out. The change in length relative to the diameter of the cylindrical stage was from 20d at the start to 8d at the end of the active phase (Fig. 7, *b*). The shape of MF was accepted as ogive with a length of 2.57d. During the flight along the active phase, the atmospheric velocity of LV ranged from 0 m/s to 2300 m/s (Fig. 7, *d*), which corresponded to M=8 (Fig. 7, *g*) at an altitude of 90 km. The angle of attack varied in the range of up to 1.62° (Fig. 7, *h*).

As can be seen from our results, the influence of the aerodynamic leads to a decrease in the flight altitude (Fig. 7, *c*) and the maximum relative speed (Fig. 7, *e*), which should have been observed. Qualitatively, the loss can be described as a shortfall based on the apparent velocity of LV of 278 m/s. At the same time, the maximum flight altitude taking into account the effect of aerodynamic resistance is 300 km compared to 372 km without its influence. In addition, there is a decrease in the maximum value of the longitudinal overload (Fig. 7, *e*), the Mach number (Fig. 7, *g*) and the angle of spatial attack (Fig. 7, *h*).

The data in Fig. 7, *a*–*c* are qualitatively similar to the data reported in [39] for the phase of work of the second stage, but taking into account the specificity of the considered LV, in particular its mass, aerodynamic characteristics, thrust force, etc.

From the data in Fig. 7, it turns out that LV under certain conditions can launch a payload of the CubeSat 24U class on a suborbital trajectory with a altitude of about 300 km. At the same time, the current longitudinal overload is 4 units, and the temperature on the surface of LV stage housing does not exceed 300 K. This indicates that there will be no significant ablation effect on the surface of LV housing, and heating of the stage housing to temperatures above 320–370 K.

Our results are correct within the framework of the accepted assumptions and the given traction equipment and geometry of LV. It should be noted that the results for thermal loads are obtained for the case of motion along a trajectory with an angle of attack close to zero. Changing one of these parameters will lead to the need for additional research.

Among the shortcomings of the current research is the issue of ensuring the integrity of LV structure under the action of overloads and heating. The main problem of polymer materials, such as polyethylene, is a significant change in the strength properties of the material when temperatures above 320–370 K are reached. Accordingly, this can lead to a loss of structural integrity. But solving this problem is not possible without defining the change ranges:

– parameters of LV motion;

– heating temperature of the surface of LV body under the influence of the force of aerodynamic resistance of the Earth's atmosphere.

On the other hand, one of the most important issues is to design an autophagic PS, the fuel for which is the polymer body of LV.

The obtained parameters of the motion of LV, and the temperature of heating on the surface of its body can be used for other parts of the task on determining the area of design parameters. Areas of further research are:

– design of autophagic PSs;

– analysis of heat and mass transfer processes in the housing on the active phase of the trajectory;

– analysis of the integrity of the hull structure under the combined influence of mechanical and thermal loads;

– analysis of the influence of heated polymer ablation on the geometry of LV and its energy capabilities;

– search for the optimal combination of polymer materials for the body;

– search for optimal launch trajectories;

– etc.

The results of our study are the basis for further development and determination of flight programs for ultra-light polymeric LVs, in particular, those using autophagic PSs.

7. Conclusions

1. A mathematical model of aerothermodynamic processes during the motion of a polymeric LV in the active phase of the flight was constructed. It comprehensively takes into account the influence of atmospheric dynamics, changes in geometry and flight mode on the aerodynamics and thermal state of LV and allows determining rational flight programs.

2. The influence of the aerodynamic force on the parameters of the motion of a variable-length ultralight-class LV made of a polymer body along the active phase of the trajectory was investigated. Qualitatively, the losses can be described by a shortfall in the apparent velocity of LV of 278 m/s and a decrease in the maximum flight altitude by 72 km.

3. The principal possibility of launching a CubeSat 24U class payload on a suborbital trajectory with a altitude of about 300 km has been shown. In this case, the longitudinal overload does not exceed 4 units while the temperature on the surface of the body does not exceed 300 K.

Conflicts of interest

The authors declare that they have no conflicts of interest in relation to the current study, including financial, personal, authorship, or any other, that could affect the study and the results reported in this paper.

Funding

The research was carried out within the framework of the project "Theoretical foundations for designing ultralight launch vehicles from polymeric materials" within the EU Framework Program for Research and Innovation "Horizon 2020"; contract RN/12-2023 with the Ministry of Education and Science of Ukraine.

Data availability

All data are available in the main text of the manuscript.

Use of artificial intelligence

The authors confirm that they did not use artificial intelligence technologies when creating the current work.

References

1. Yemets, V., Sanin, F., Dzhur, Y., Masliany, M., Kostritsyn, O., Minteev, G. (2009). Single-stage small satellite launcher with combustible tank of polyethylene. Acta Astronautica, 64 (1), 28–32. https://doi.org/10.1016/j.actaastro.2008.06.015
2. Yemets, V., Sanin, F., Masliany, M., Kostritsyn, O., Minteev, G. (2010). Is the combustible inertial pico launch vehicle feasible? JBIS - Journal of the British Interplanetary Society, 63 (7), 249–259.
3. Yemets, V., Harkness, P., Dron', M., Pashkov, A., Worrall, K., Middleton, M. (2018). Autophage Engines: Toward a Throttleable Solid Motor. Journal of Spacecraft and Rockets, 55 (4), 984–992. https://doi.org/10.2514/1.a34153
4. Dron, M. M., Dubovyk, L. H., Holubek, O. V., Dreus, A. Yu., Yemets, A. V., Pashkov, A. V. (2019). Systemy vidvodu kosmichnykh obiektiv z nyzkykh navkolozemnykh orbit. Dnipro: LIRA, 218.
5. Yemets, V., Dron, M., Pashkov, A., Dreus, A., Kositsyna, Ye., Yemets, M. et al. (2020). Method to preset G-load profile of launch vehicles. Proceedings of the International Astronautical Congress, IAC.
6. Yemets, V., Dron', M., Pashkov, A. (2020). Autophage Engines: Method to Preset Gravity Load of Solid Rockets. Journal of Spacecraft and Rockets, 57 (2), 309–318. https://doi.org/10.2514/1.a34597
7. Yemets, V., Dron, M., Dreus, A., Pashkov, A., Yemets, M. (2021). Heat flows in the gasification chamber of the polymer propelled autophage launch vehicle. Proceedings of the International Astronautical Congress.
8. Dreus, A., Yemets, V., Dron, M., Yemets, M., Golubek, A. (2021). A simulation of the thermal environment of a plastic body of a new type of launch vehicle at the atmospheric phase of the trajectory. Aircraft Engineering and Aerospace Technology, 94 (4), 505–514. https://doi.org/10.1108/aeat-04-2021-0100
9. Dreus, A. Yu., Dron, M. M., Dubovik, L. G., Strembovsky, V. V. (2023). Assessment of the possibility of using polymers in the bodies of promising launch vehicles based on the heat resistance factor. Space Science and Technology, 29 (6), 03–12. https://doi.org/10.15407/knit2023.06.003
10. Kondratiev, A. V. (2020). A concept of optimization of structural and technological parameters of polymer composite rocket units considering the character of their production. Space Science and Technology, 26 (6), 5–22. https://doi.org/10.15407/knit2020.06.005
11. Kondratiev, A. V., Kovalenko, V. O. (2019). Optimization of design parameters of the main composite fairing of the launch vehicle under simultaneous force and thermal loading. Science and Technology, 25 (4), 3–21. https://doi.org/10.15407/knit2019.04.003
12. Kondratiev, A., Potapov, O., Tsaritsynskyi, A., Nabokina, T. (2021). Optimal Design of Composite Shelled Sandwich Structures with a Honeycomb Filler. Advances in Design, Simulation and Manufacturing IV, 546–555. https://doi.org/10.1007/978-3-030-77719-7_54

13. Kositsyna, O. S., Dron', M. M., Yemets, V. V. (2020). The environmental impact assessment of emission from space launches: the promising propellants components selection. Journal of Chemistry and Technologies, 28 (2), 186–193. https://doi.org/10.15421/082020
14. Kositsyna, O., Varlan, K., Dron, M., Kulyk, O. (2021). Determining energetic characteristics and selecting environmentally friendly components for solid rocket propellants at the early stages of design. Eastern-European Journal of Enterprise Technologies, 6 (6 (114)), 6–14. https://doi.org/10.15587/1729-4061.2021.247233
15. Wang, L., He, G. Y., Wang, Q., Chen, L. S. (2020). An Engineering Method for Computing the Aerodynamics Performance of Hypersonic Vehicle. IOP Conference Series: Materials Science and Engineering, 816 (1), 012006. https://doi.org/10.1088/1757-899x/816/1/012006
16. Yang, Z., Wang, S., Gao, Z. (2022). Studies on effects of wall temperature variation on heat transfer in hypersonic laminar boundary layer. International Journal of Heat and Mass Transfer, 190, 122790. https://doi.org/10.1016/j.ijheatmasstransfer.2022.122790
17. Zhao, M. (2021). Prediction and Validation Technologies of Aerodynamic Force and Heat for Hypersonic Vehicle Design. In Springer Aerospace Technology. Springer Singapore. https://doi.org/10.1007/978-981-33-6526-1
18. Dillenius, M. F. E., Nielsen, J. N. (1979). Computer Programs for Calculating Pressure Distributions Including Vortex Effects on Supersonic Monoplane or Cruciform Wing-Body-Tail Combinations with Round or Elliptical Bodies. NASA. Available at: https://ntrs.nasa.gov/citations/19810018506
19. Cengizci, S., Uğur, Ö., Takizawa, K., Tezduyar, T. (2020). A Streamline-Upwind/Petrov-Galerkin Formulation For Supersonic and Hypersonic Flow Simulations. The 20th Biennial Computational Techniques and Applications Conference (CTAC2020). Available at: http://hdl.handle.net/11511/94032
20. Li, J., Jiang, D., Geng, X., Chen, J. (2021). Kinetic comparative study on aerodynamic characteristics of hypersonic reentry vehicle from near-continuous flow to free molecular flow. Advances in Aerodynamics, 3 (1). https://doi.org/10.1186/s42774-021-00063-0
21. Huang, T., He, G., Wang, Q. (2022). Calculation of Aerodynamic Characteristics of Hypersonic Vehicles Based on the Surface Element Method. Advances in Aerospace Science and Technology, 07 (02), 112–122. https://doi.org/10.4236/aast.2022.72007
22. Furudate, M. A. (2022). MC-New: A Program to Calculate Newtonian Aerodynamic Coefficients Based on Monte-Carlo Integration. Aerospace, 9 (6), 330. https://doi.org/10.3390/aerospace9060330
23. Thomas, P. D., Vinokur, M., Bastianon, R. A., Conti, R. J. (1972). Numerical Solution for Three-Dimensional Inviscid Supersonic Flow. AIAA Journal, 10 (7), 887–894. https://doi.org/10.2514/3.50241
24. Hussein, A. K, Khan, W. A., Sivasankaran, S., Mohammed, H. A., Adegun, I. K. (2013). Numerical simulation of three-dimensional supersonic flow around an aerodynamic bump. Journal of Basic and Applied Scientific Research, 3 (7), 656–666.
25. Marchenay, Y., Olazabal Loumé, M., Chedevergne, F. (2022). Hypersonic Turbulent Flow Reynolds-Averaged Navier–Stokes Simulations with Roughness and Blowing Effects. Journal of Spacecraft and Rockets, 59 (5), 1686–1696. https://doi.org/10.2514/1.a35339
26. Sofair, I. (1995). Improved Method for Calculating Exact Geodetic Latitude and Altitude. Defense Technical Information Center. https://doi.org/10.21236/ada294568
27. Bin, Y., Huang, G., Kunz, R., Yang, X. I. A. (2024). Constrained Recalibration of Reynolds-Averaged Navier–Stokes Models. AIAA Journal, 62 (4), 1434–1446. https://doi.org/10.2514/1.j063407
28. Prihod'ko, A. A. (2008). Komp'yuternye tehnologii v aerogidrodinamike i teplomassoobmene. Kyiv: NAUKOVA DUMKA, 380.
29. Prykhodko, O. A., Alekseyenko, S. V. (2014). Numerical simulation of the process of airfoil icing in the presence of large supercooled water drops. Technical Physics Letters, 40 (10), 864–867. https://doi.org/10.1134/s1063785014100125
30. Prikhod'ko, A. A., Alekseenko, S. V. (2014). Numerical Simulation of the Processes of Icing on Airfoils with Formation of a "Barrier" Ice. Journal of Engineering Physics and Thermophysics, 87 (3), 598–607. https://doi.org/10.1007/s10891-014-1050-0
31. Alekseyenko, S., Dreus, A., Dron, M., Brazaluk, O. (2022). Numerical Study of Aerodynamic Characteristics of a Pointed Plate of Variable Elongation in Subsonic and Supersonic Gas Flow. Journal of Advanced Research in Fluid Mechanics and Thermal Sciences, 96 (2), 88–97. https://doi.org/10.37934/arfmts.96.2.8897
32. Gutiérrez, R., Llorente, E., Ragni, D., Aranguren, P. (2022). Study on k–ω–Shear Stress Transport Corrections Applied to Airfoil Leading-Edge Roughness Under RANS Framework. Journal of Fluids Engineering, 144 (4). https://doi.org/10.1115/1.4052925
33. Adanta, D., Fattah, I. M. R., Muhammad, N. M. (2020). Comparison of standard k-epsilon and SST k-omega turbulence model for breastshot waterwheel simulation. Journal of Mechanical Science and Engineering, 7 (2), 039–044. https://doi.org/10.36706/jmse.v7i2.44
34. Costa, L. M. F., Montiel, J. E. S., Corrêa, L., Lofrano, F. C., Nakao, O. S., Kurokawa, F. A. (2022). Influence of standard k-ε, SST κ-ω and LES turbulence models on the numerical assessment of a suspension bridge deck aerodynamic behavior. Journal of the Brazilian Society of Mechanical Sciences and Engineering, 44 (8). https://doi.org/10.1007/s40430-022-03653-1
35. Maurício Araújo, A., Antônio Coutinho Silva, A., Leal dos Santos, C., Corte Real Fernandes, E., Menezes, E., José Arruda Moura Rocha, G. et al. (2017). An assessment of different turbulence models on a CFD simulation of air flow past a S814 airfoil. Procceedings of the 24th ABCM International Congress of Mechanicl Engineering. https://doi.org/10.26678/abcm.cobem2017.cob17-0306
36. Robinson, D., Hassan, H. (1996). A two-equation turbulence closure model for wall bounded and free shear flows. Fluid Dynamics Conference. https://doi.org/10.2514/6.1996-2057
37. Petrov, K. P. (1998). Aerodinamika tel prosteyshih form. Moscow: Fizmatlit, 428.
38. Meng, Y., Yan, L., Huang, W., Tong, X. (2020). Numerical Investigation of the Aerodynamic Characteristics of a Missile. IOP Conference Series: Materials Science and Engineering, 887 (1), 012001. https://doi.org/10.1088/1757-899x/887/1/012001
39. Bayley, D. J., Hartfield, R. J., Burkhalter, J. E., Jenkins, R. M. (2008). Design Optimization of a Space Launch Vehicle Using a Genetic Algorithm. Journal of Spacecraft and Rockets, 45 (4), 733–740. https://doi.org/10.2514/1.35318